AD-A065 322 VARIAN ASSOCIATES INC PALO ALTO CA F/G 20/12
INVESTIGATION OF INP TECHNOLOGY.(U)
JAN 79 G A ANTYPAS F19628-77-C-0141
UNCLASSIFIED SCIENTIFIC-1 RADC-TR-78-286 NL

1 OF 1
AD A065322

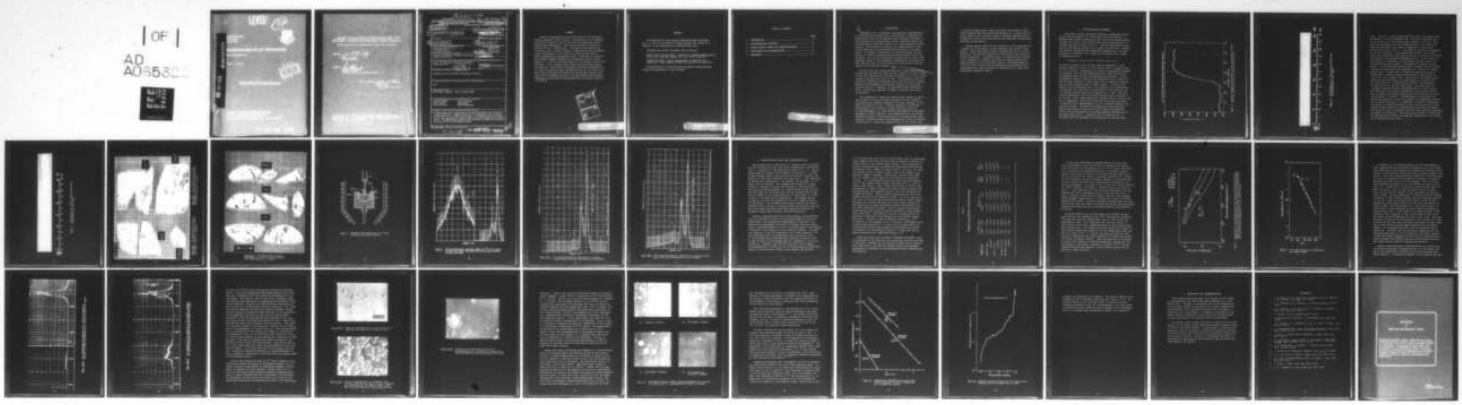

END
DATE FILMED
4 -79
DDC

LEVEL II

12

RADC-TR-79-266
Interim Report
January 1979

INVESTIGATION OF InP TECHNOLOGY

Varian Associates, Inc.

George A. Antypas

DDC
DECEMBER
DEC 27 1979
C

DDC FILE COPY

AD A065322

This report has been reviewed by the RADC Information Office (OI) and is releasable to the National Technical Information Service (NTIS). At NTIS it will be releasable to the general public, including foreign nations.

RADC-TR-78-286 has been reviewed and is approved for publication.

APPROVED: John K. Kennedy

JOHN K. KENNEDY
Contract Monitor

APPROVED: [illegible]

[illegible]
Director, Solid State Sciences Division

FOR THE COMMANDER: John P. Huss

JOHN P. HUSS
Acting Chief, Plans Office

(9) Interim Rept. 1 Aug 77 - 1 Aug 78

UNCLASSIFIED

SECURITY CLASSIFICATION OF THIS PAGE (When Data Entered)

(19) REPORT DOCUMENTATION PAGE

READ INSTRUCTIONS BEFORE COMPLETING FORM

(18) 1. REPORT NUMBER: RADC-TR-78-286	2. GOVT ACCESSION NO. — 3. RECIPIENT'S CATALOG NUMBER
(6) 4. TITLE (and Subtitle): INVESTIGATION OF InP TECHNOLOGY.	(14) 5. TYPE OF REPORT & PERIOD COVERED: Scientific [illegible] No. 1; 1 Aug 77 - 1 Aug 78
	6. PERFORMING ORG. REPORT NUMBER: N/A
(10) 7. AUTHOR(s): George A. Antypas	(15) 8. CONTRACT OR GRANT NUMBER(s): F19628-77-C-0141
9. PERFORMING ORGANIZATION NAME AND ADDRESS: Varian Associates, Inc. 611 Hansen Way Palo Alto CA 94303	10. PROGRAM ELEMENT, PROJECT, TASK AREA & WORK UNIT NUMBERS: (16) 61102F 2306J124 (17) J1
11. CONTROLLING OFFICE NAME AND ADDRESS: Deputy for Electronic Technology (RADC/ESM) Hanscom AFB MA 01731	(11) 12. REPORT DATE: Jan[illegible]1979; 13. NUMBER OF PAGES: 33
14. MONITORING AGENCY NAME & ADDRESS (if different from Controlling Office): Deputy for Electronic Technology (RADC/ESM) Hanscom MA 01731 (12) 39p.	15. SECURITY CLASS. (of this report): UNCLASSIFIED; 15a. DECLASSIFICATION/DOWNGRADING SCHEDULE: N/A

16. DISTRIBUTION STATEMENT (of this Report)

Approved for public release; distribution unlimited.

17. DISTRIBUTION STATEMENT (of the abstract entered in Block 20, if different from Report)

Same

18. SUPPLEMENTARY NOTES

RADC Project Engineer: John K. Kennedy (ESM)

19. KEY WORDS (Continue on reverse side if necessary and identify by block number)

indium phosphide	solution growth
single crystal	high purity
polycrystalline	photoluminescence

20. ABSTRACT (Continue on reverse side if necessary and identify by block number)

Extremely high purity polycrystalline InP has been prepared from solution at 2 cm/day growth rate. Single-crystal InP with background carrier concentration of less than 1×10^{15}/cc was prepared. Low temperature PL measurements on both poly and single InP indicate materials quality comparable to epitaxial layers. Zinc-doped single crystals having extremely low dislocation density, less than $10^3/cm^2$, are routinely prepared.

DD FORM 1 JAN 73 1473 EDITION OF 1 NOV 65 IS OBSOLETE

UNCLASSIFIED

SECURITY CLASSIFICATION OF THIS PAGE (When Data Entered)

5/N 364 100

79 08 02 000

SUMMARY

Growth of polycrystalline InP from solution can be reproducibly prepared in 450-g ingots. The material is of extremely high purity, based on Van der Pauw and low temperature photoluminescence measurements. The growth process is capable of growing InP at a 2 cm/day rate. Increase of the growth rate to greater than 2 cm/day results in undesirable nonstoichiometry levels, detrimental in the growth of single-crystal InP by liquid encapsulation Czochralski (LEC). LEC-grown InP crystals when undoped exhibit extremely low background carrier concentration $< 1 \times 10^{15}$/cc and mobilities at 77°K greater than 51,000 cm^2/V-sec. This represents the highest purity single-crystal InP reported. The effect of doping on structural imperfections of single crystals has been investigated for Sn, Fe, and Zn; in every case a decrease was observed in dislocation density compared with the undoped crystals, and particularly the Zn-doped crystals were practically dislocation-free for doping levels of 2×10^{18}/cc.

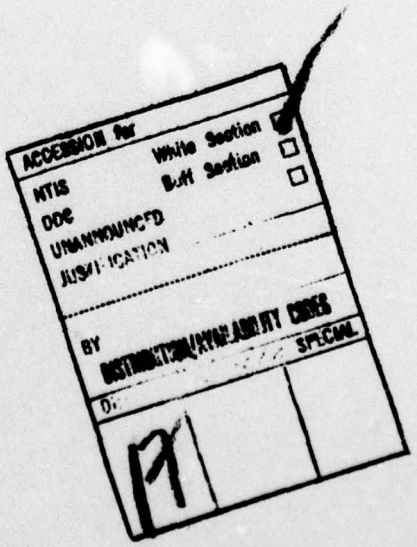

PREFACE

Contributions to the research described herein were made by C. L. Wei in the growth of single-crystal InP, and by M. L. Simkins in the preparation of polycrystalline InP.

Previous and related contracts are as follows:

N00123-76-C-1312 and 0416: "InGaAsP for Infrared Applications," Naval Ocean Systems Command, CA, June 1976 to Aug 1977.

DAAG29-76-C-0015: "Basic Improvements in Substrate InP Materials," Army Research Office, SC, Feb 1976 to Jan 1978.

No publications or articles have resulted to date from the research accomplished on this contract.

TABLE OF CONTENTS

1. INTRODUCTION

Undoubtedly InP is becoming a very important semiconductor, in particular for optoelectronic applications. Although InP-based device results are appearing with increased frequency in both microwave and optoelectronic areas, substrate growth and characterization have been limited to a few government contract reports. This program is aimed at the investigation of InP-based technology from polycrystalline synthesis to epitaxial growth. Of primary consideration is the development of technology for reliably synthesizing polycrystalline InP from the elements. Even though the growth of single-crystal InP is well developed, based on the commercial equipment for LEC-growth of GaAs and GaP, very little information is available on the synthesis of InP from the elements.

InP has long been recognized as being a semiconductor with interesting applications possibilities, similar to those of GaAs; it was also realized that the partial pressure of P at the stoichiometric melting point was 27.5 atm. This property alone prevented the commercial development of InP devices until recently. Synthesis and Bridgman single-crystal growth of InP had been reported earlier.[1] However, the experiments were performed in small, thick-walled ampoules in order to minimize the danger of explosion.

The technology of large InP single-crystal growth by LEC is very similar to that previously developed for GaP; therefore polycrystalline synthesis remained as the main obstacle in the ready availability of InP. Similar problems of course were encountered in the synthesis of GaP; these were resolved by the development of a high pressure polycrystalline synthesis equipment by Metals Research, and alternatively by the Frosch technique (growth of GaP from solution in an open system under flowing P, obtained either from decomposition of PH_3 or evaporation of red P). Since the solubility of P in Ga is very low

at moderate temperatures, these techniques have apparent advantages compared with the growth from solution in a closed system. In the case of InP, solution growth at moderate temperatures can potentially yield InP of high quality and excellent stoichiometry required for LEC growth.

Single-crystal growth of InP basically is well developed for it makes use of processes initially used for the growth of GaP. However, areas that require closer investigation are the purity, electrical, and optical properties of the crystal and crystallographic perfection. Characterization of single crystals include x-ray topography in studying the effect of doping species and doping density on the dislocation density, photoluminescence at 77°K and 1.8°K, Van der Pauw measurements and photocapacitance measurements for identification and concentration of deep lying nonradiative impurity levels.

2. POLYCRYSTALLINE SYNTHESIS

Work under earlier government contracts established preliminary growth parameters for polycrystalline InP synthesis. A Bridgman-type system consisting of two 36-inch resistance-heated furnaces was set up, with each furnace controlled separately to produce the profile shown in Fig. 1. The low temperature region controls the partial pressure of P during the reaction. Backmann and Buehler[2] determined the temperature dependence of the vapor pressure of commercial red P (which was obtained from a number of suppliers) to be

$$\ell n\ P(atm) = -(10.8 \pm 0.4) \times 10^3/T + 16.5 \pm 0.6 \quad .$$

At 400°C the error limits of this equation represent a total pressure range of 0.5 to 5.57 atm, and at 450°C a pressure range of 0.6 to 15 atm. Undoubtedly this range is appreciably narrower for material from the same manufacturer provided the material is prepared under reliable and reproducible processes. A very satisfactory source of high purity commercial red P is MCP, Ltd. The findings presented in this report were exclusively obtained with In and P procured from the above source. Initally, the reactor tube was designed for a 450-g charge, to be synthesized from solution at 1000°C and P controlled at 400°C resulting in a P partial pressure during the reaction of ~ 3 atm. The temperature gradient at the solid liquid interface was estimated to be 15°C/cm. Under these conditions a growth rate of 1 cm per day can be supported. Since the In boat was 30 cm long and having a cross-section of approximately 3 cm^2, a complete synthesis run required 30 days. The material obtained was polycrystalline having grain size as large as 0.5 cm^2, highly stoichiometric, and as will be discussed in the characterization section was of extremely high purity. A typical ingot is shown in Fig. 2. Obviously the main drawback of this approach is the low yield

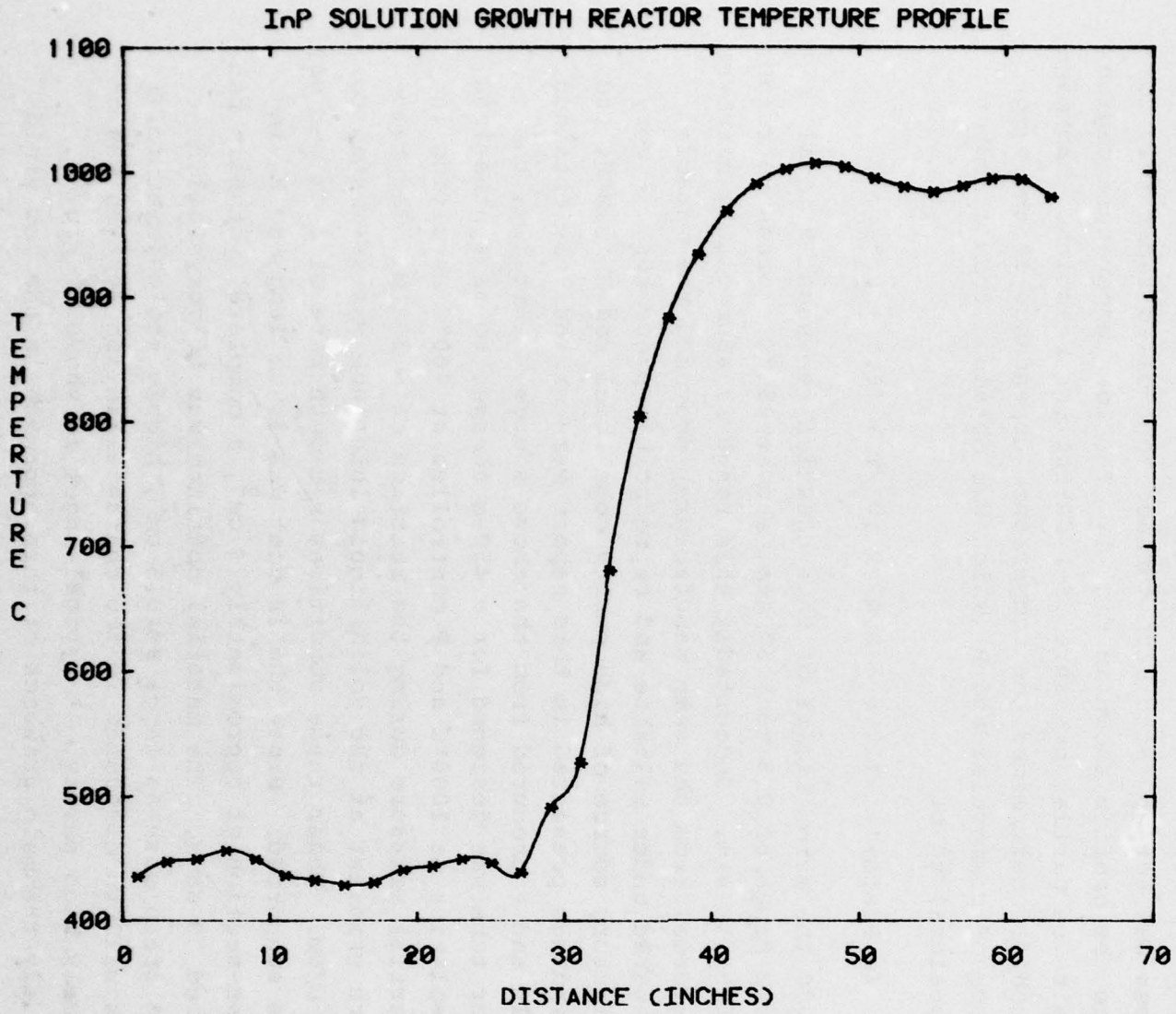

Fig. 1. Typical temperature profile in the horizontal reactor for the solution growth of polycrystalline InP.

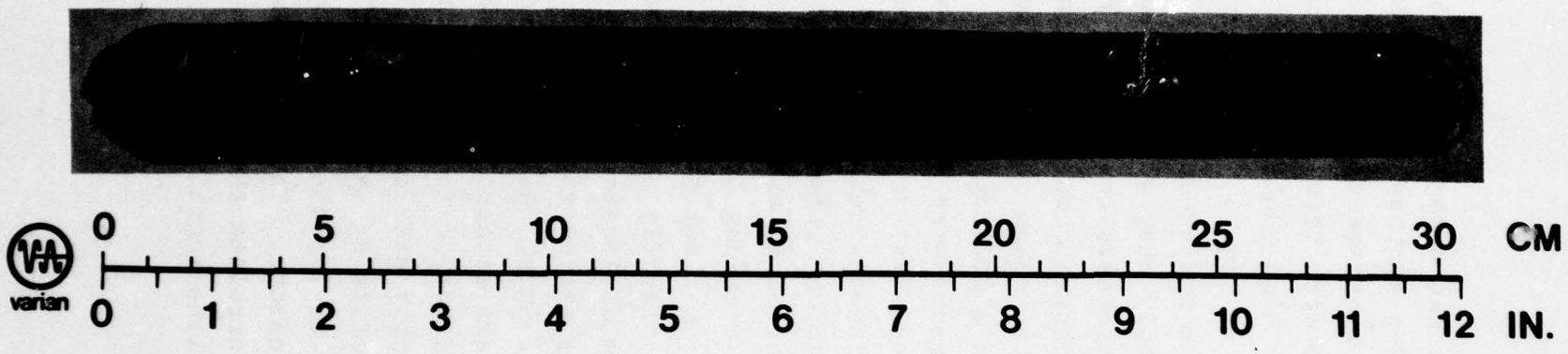

Fig. 2. Photograph of a 430-g polycrystalline solution-grown InP ingot.

rate. Initially it was thought that the reactor and charge could be scaled to a 1500-g synthesis run. The boat length was kept at 30 cm while the cross-section was increased to 10 cm^2. Four runs were performed with this reactor design: two yielded material of extremely high quality, comparable to the earlier 450-g runs as seen in Fig. 3. Two however resulted in explosions. It is very difficult to investigate the cause(s) of the explosions, but undoubtedly they were related to the reactor size and/or the reactor wall thickness-to-diameter ratio. In any event, it was decided to concentrate on the original reactor design and investigate alternate means in increasing the capacity of the system. An obvious modification was to increase the travel rate. A series of experiments were performed at 4 cm/day and 2 cm/day growth rates. Figure 4(a)-(c) shows low magnification photomicrographs of polished wafers obtained from ingots grown at 1 cm, 2 cm, and 4 cm/day rates. As expected, the highest stoichiometry was exhibited by the ingot grown at 1 cm/day, while the ingot grown at 4 cm/day had the highest nonstoichiometry in addition to the smallest grain size. The ingot grown at 2 cm/day--although slightly nonstoichiometric--is well suited for high purity low dislocation density single-crystal growth. Thus at present the system capacity has been optimized to yield approximately 1 kg/month. Alternate means of increasing the system throughput are either to increase the temperature gradient at the growth interface or to increase the reaction temperature. The former is probably difficult to do, since we arrived at the present thermal profile by extensive trial-and-error procedures. The latter is easy to implement, although care should be exercised in preventing explosions. This is an area we plan to investigate and particularly correlate the reaction temperature to the purity of the polycrystalline ingot.

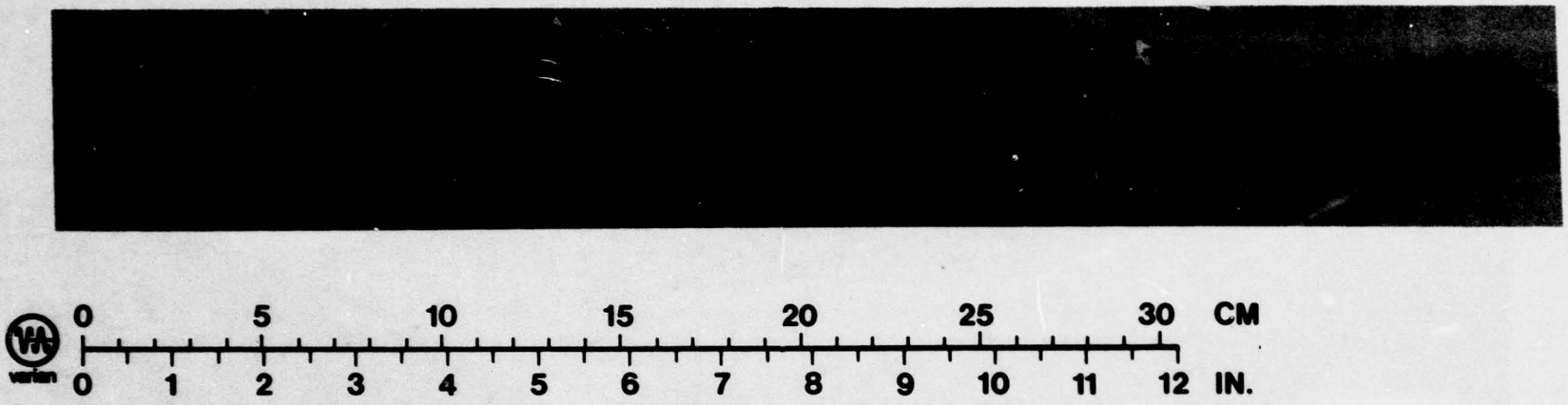

Fig. 3. Photograph of a 1500-g polycrystalline solution-grown InP ingot.

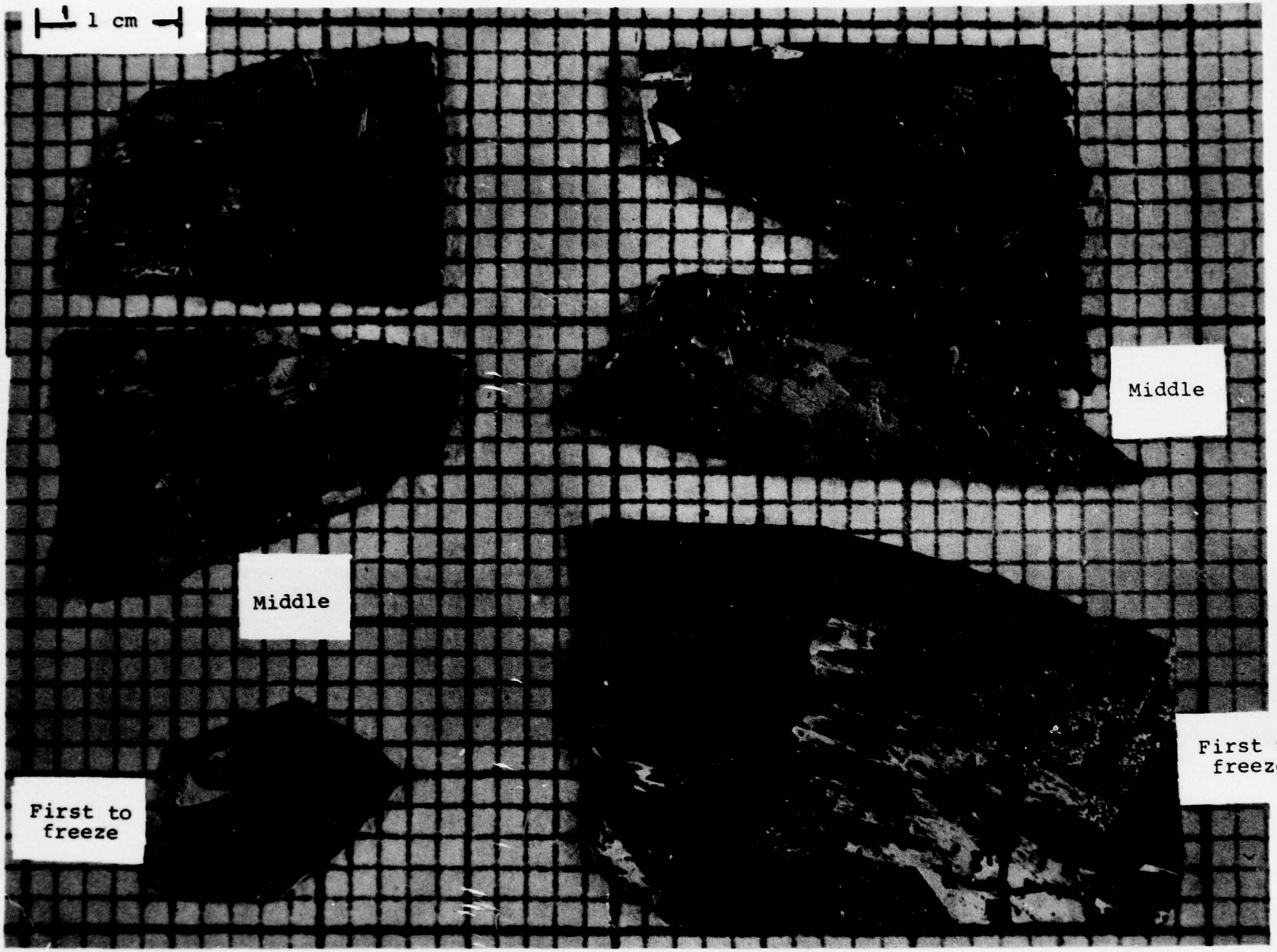

Fig. 4(a). Low magnification photomicrograph of wafers from polycrystalline ingot grown at 1 cm/day.

Fig. 4(b). Low magnification photomicrograph of wafers from polycrystalline ingot grown at 4 cm/day.

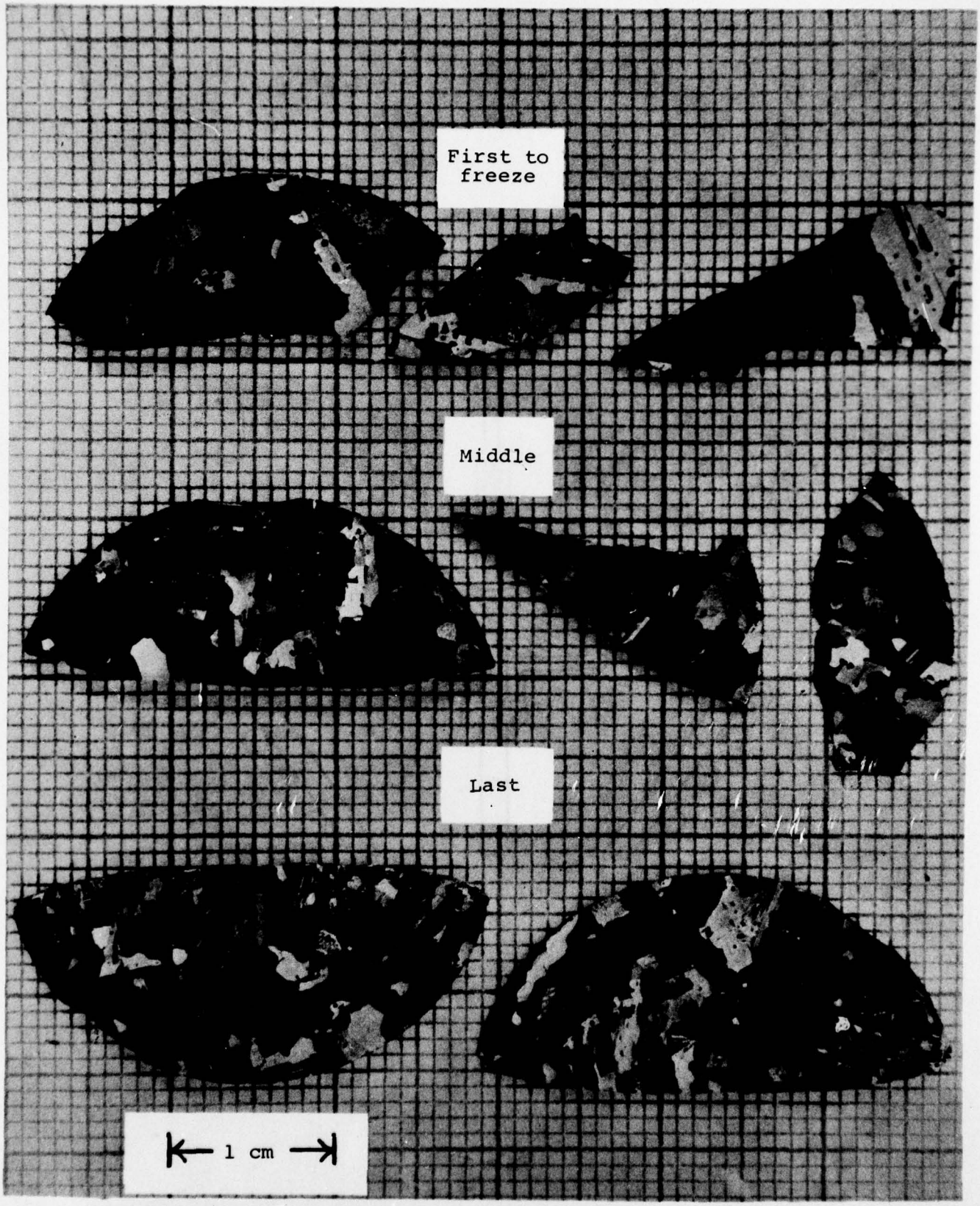

Fig. 4(c). Low magnification photomicrograph of wafers from polycrystalline ingot grown at 2 cm/day.

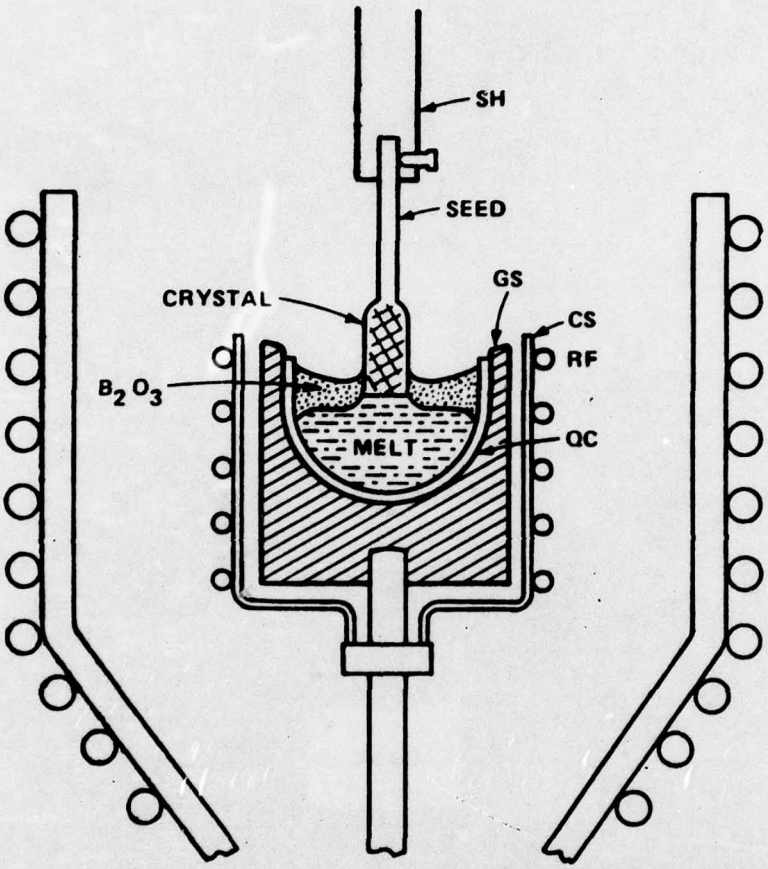

Fig. 5. Schematic representation of a high pressure LEC crystal puller.

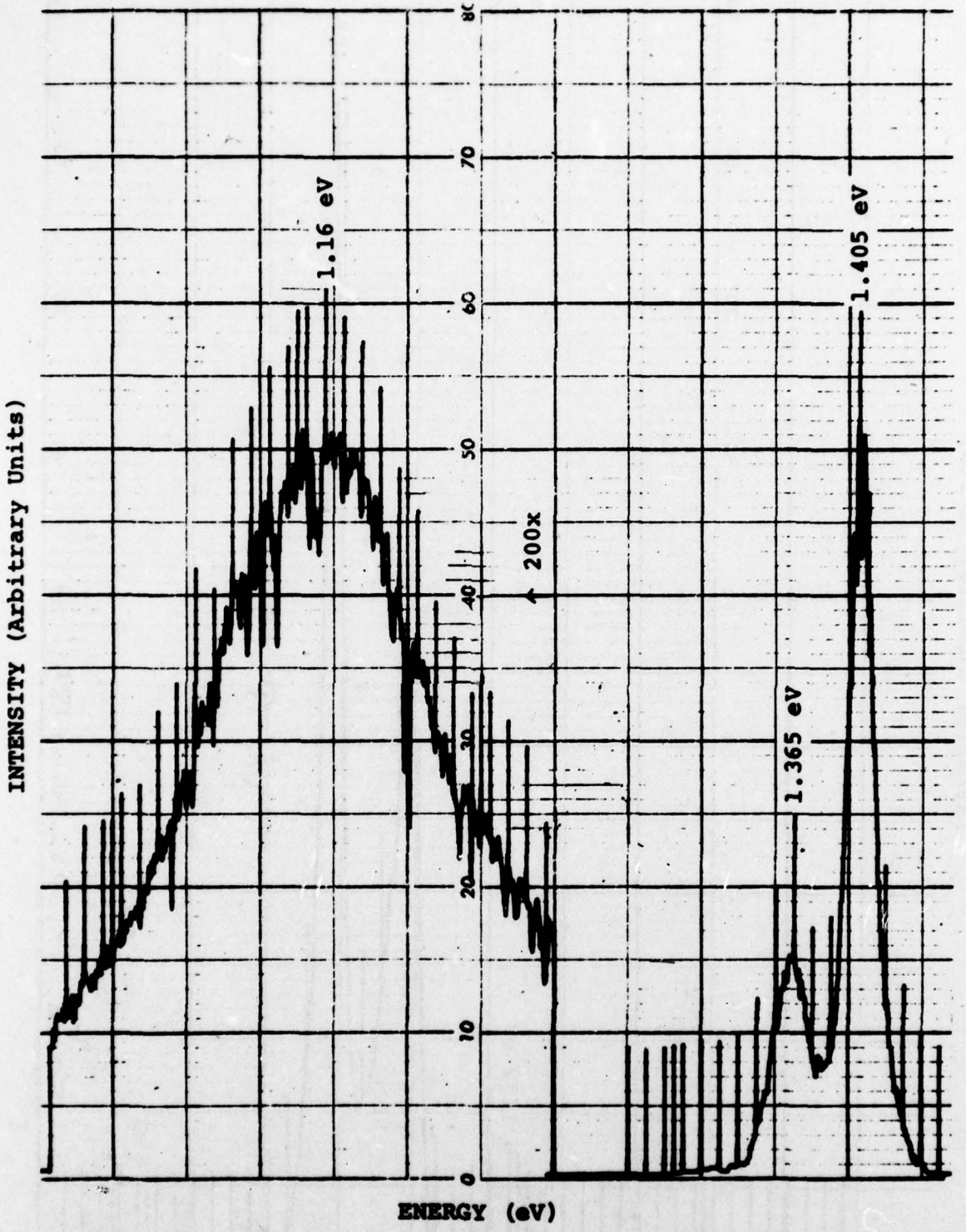

Fig. 6. Photoluminescence spectrum taken at 77°K of a polycrystalline wafer obtained from the first portion of poly InP VA#7.

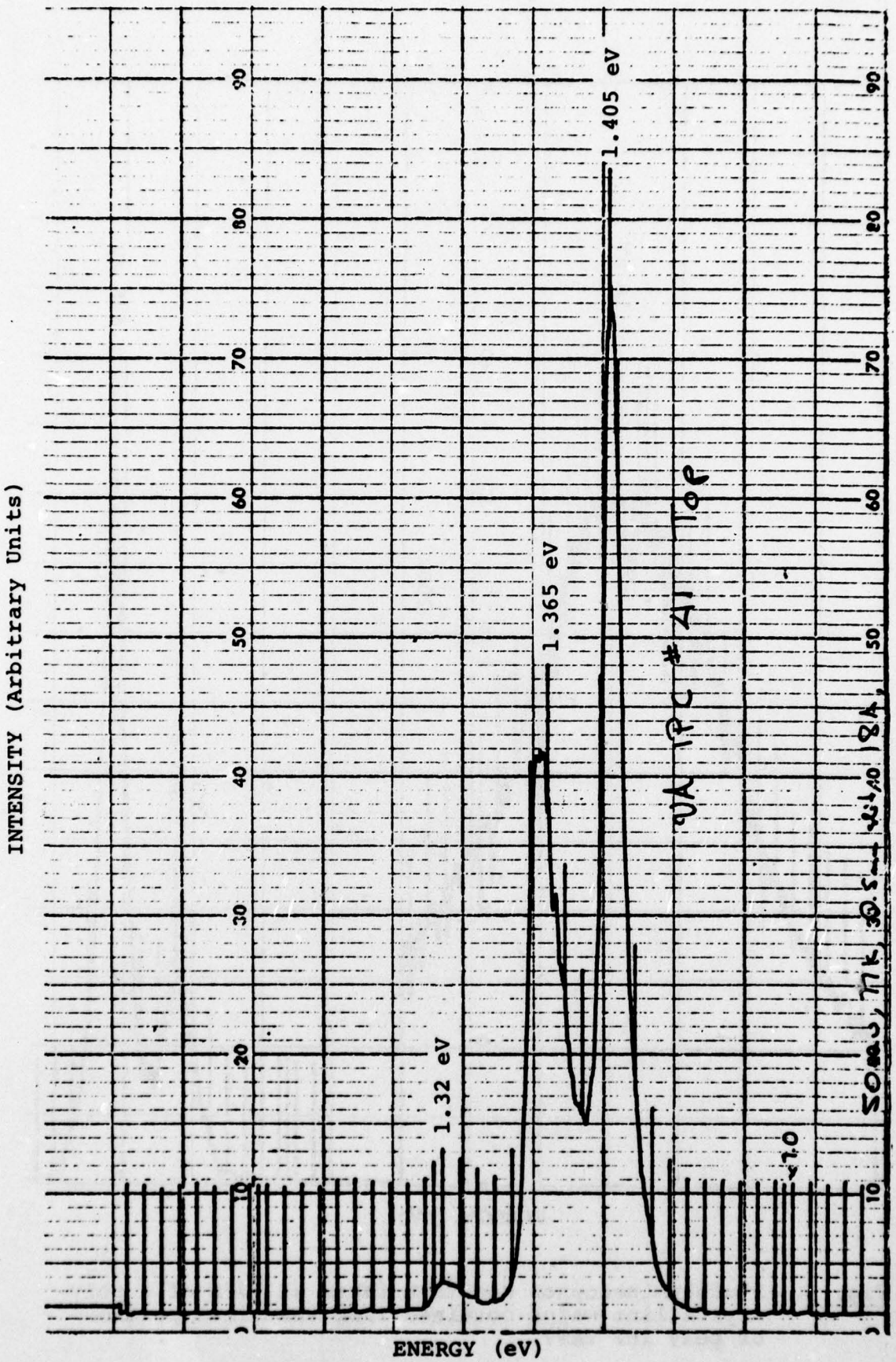

Fig. 7(a). 77°K photoluminescence spectrum of a single crystal wafer from the top portion of VA-IPC#41.

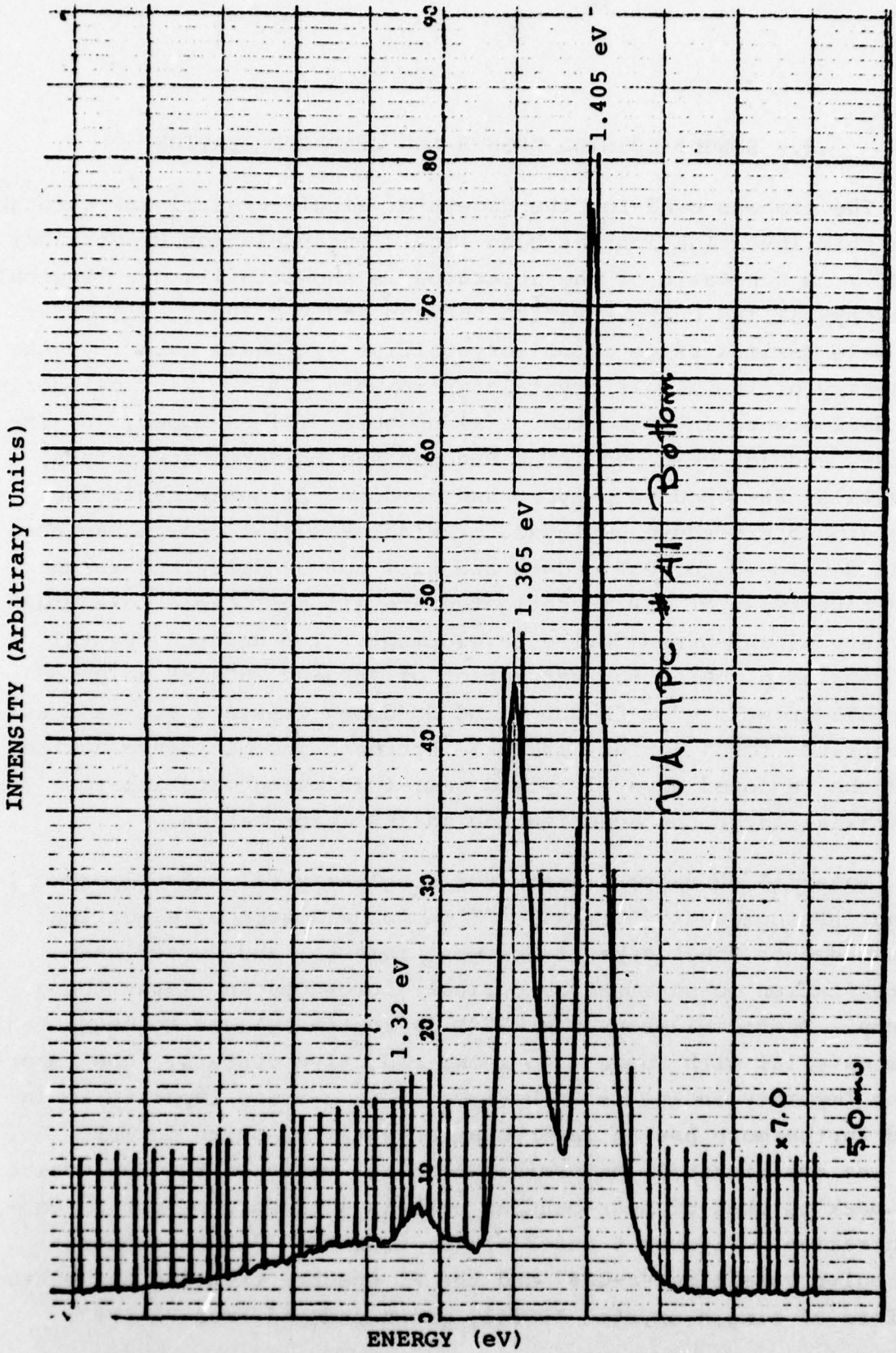

Fig. 7(b). 77°K photoluminescence spectrum of a single-crystal wafer from the bottom portion of VA-IPC#41.

3. SINGLE-CRYSTAL GROWTH AND CHARACTERIZATION

The process used for the growth of single-crystal InP throughout this investigation has been liquid encapsulation Czochralski (LEC). A schematic of the apparatus is shown in Fig. 5. Typical polycrystalline charges varied between 450 and 200 g. In order to make maximum usage of polycrystalline synthesis capacity, the majority of the single crystals grown were 200 g. Four categories of doping were investigated: (a) undoped, (b) Sn-doped, (c) Zn-doped, and (d) Fe-doped. The undoped and Sn-doped are n-type crystals, Zn-doped is p-type, and Fe-doped is semi-insulating. The growth procedure employed for single-crystal growth has been well developed for GaP growth and will not be described further. The four types of InP investigated are all applicable to a wide variety of InP-based device development. The undoped crystal is used as a source for saturation of InP and InGaAsP solution for LPE growth. The Zn-doped and Sn-doped crystals are used as substrates for a variety of optoelectronic and microwave devices, and the Fe-doped crystals yield semi-insulating material for epitaxial layer characterization and FET fabrication.

Material characterization for single-crystal and polycrystalline InP included 77°K and 1.8°K photoluminescence, electrical measurements, photocapacitance measurements, and defect characterization measurement by optical microscopy and x-ray topography. Photoluminescence at 77°K is routinely used to characterize the material with respect to known radiative centers. One important impurity in InP is Zn because it is a trace impurity in In and furthermore has an incorporation ratio of unity in InP. It was qualitatively determined that the ratio of the Zn level PL peak to that of near-bandgap peak is a measure of the Zn concentration. Figures 6 and 7(a)-(b) show the 77°K PL spectra of polycrystalline VA-GF#7 and the PL spectra from top and bottom wafers of single-crystal IPC#41, grown undoped from VA-GF#7.

It is obvious that the 1.365 to 1.405-eV peak ratio is appreciably lower compared with that obtained from PL spectra of the top and bottom wafers of the IPC#41 single crystal. This difference is probably associated with increased Zn contamination potentially originating from a number of sources such as (a) B_2O_3, (b) since the crystal puller is used for both n and p-type growth, high pressure chamber, susceptor, seed holder, and any other parts that are common to both types of runs could be contamination sources. It is gratifying however that the electrical measurement of the undoped single crystal indicates that it is of extremely high purity. Table I shows the results of Van der Pauw measurements of IPC#17 undoped InP single crystal prepared with polycrystalline InP obtained from MCP, Ltd. and the results of VA-GF#2 and IPC#41. Solution-grown polycrystalline InP is the highest purity bulk InP reported to date. It is of interest to note that in both the polycrystalline and single-crystal ingots prepared with in-house InP poly the first-to-grow sections of the ingots are of higher background carrier concentration than the later solidifying sections. This is unusual since during solidification most impurities have distribution coefficients K lower than unity. This behavior can only be explained by the presence of impurities with distribution coefficients greater than unity. Silicon is such an impurity, having $K_{Si} = 30$.[3] In addition to the presence of Si in the melt, the concentration of other impurities with $K < 1$ have to be of sufficiently low concentration so that the increase in concentration of impurities ahead of the solidifying interface is lower than the decrease associated with impurities having $K > 1$.

IPC#17 was grown under identical conditions as IPC#41, with the exception of the source of polycrystalline InP which was MCP. In this case, although the top section of IPC#17 was of sufficiently high purity, the last-to-solidify section had degraded appreciably as reflected by the background carrier concentration and mobility.

TABLE I

RESULTS OF ELECTRICAL CHARACTERIZATION

Sample No.	μ (cm^2/V-sec) 300°K	μ (cm^2/V-sec) 77°K	$(N_D - N_A)$/cc 300°K	$(N_D - N_A)$/cc 77°K	N_D^+/cc 300°K	N_A^-/cc 77°K
IPC#17 (top)	4930	23240	5.7×10^{15}	4.9×10^{15}	7.4×10^{15}	2.5×10^{15}
" (bottom)	3410	15620	5.5×10^{15}	7.0×10^{15}	1.4×10^{16}	7.1×10^{15}
IPC#41 (top)	4671	42645	2.3×10^{15}	2.1×10^{15}	2.6×10^{15}	5.3×10^{14}
" (bottom)	4664	52793	1.1×10^{15}	9.7×10^{14}	1.4×10^{15}	3.9×10^{14}
VA-GF#1 (first)	5966	90890	6.9×10^{14}	6.8×10^{14}	---	---
VA-GF#2 (first)	5282	76680	8.5×10^{14}	8.1×10^{14}	---	---
" (middle)	5870	85960	4.4×10^{14}	4.2×10^{14}	---	---

Van der Pauw measurements yielding mobility and net electron concentration can be used along with theoretically determined variations of the mobility vs n at 77°K to give information as to the purity and compensation ratio of the grown crystal. Figure 8 shows the variation of the liquid nitrogen mobility of InP vs n calculated by workers at Mullard Laboratories.[4] Details of the calculation are not available; however it is assumed that the main effects included are ionized impurity scattering and lattice scattering. Also shown in Fig. 8 are the results obtained for IPC#17, VA-GF#1, and IPC#41. Detailed results are shown in Table I. The concentration of N_D^+ and N_A^- was determined from the compensation ratios obtained from Fig. 8 and the fact that $n = N_D - N_A$. Analysis of the results indicate that the total compensating acceptor concentration is a factor of 20 lower for IPC#41 compared with IPC#17. The main difference between these two crystals was the fact that IPC#17 was grown from an MCP polycrystalline charge while IPC#41 was grown from polycrystalline InP prepared at Varian.

The dark conductivity and Hall mobility of IPC#41 was measured between room temperature and 77°K. The electron concentration does not vary with temperatures (300 to 77°K) within the experimental error. This indicates that the donor levels are very shallow, since lower temperature does not cause appreciable donor deionization. The electron mobility varies with a power of the absolute temperature around 2.2 in the temperature range 130-300°K as shown in Fig. 9. Similar variations of mobility with respect to temperature have been reported by Glickman and Weiser[5] for n-type InP single crystals. There the mobility was analyzed in terms of two dominant scattering mechanisms (lattice and ionized impurity scattering), assuming a variation of T^{-2} for the lattice scattering as observed in their purest crystal with LN mobility = 23400 $cm^2/V\text{-sec}$.

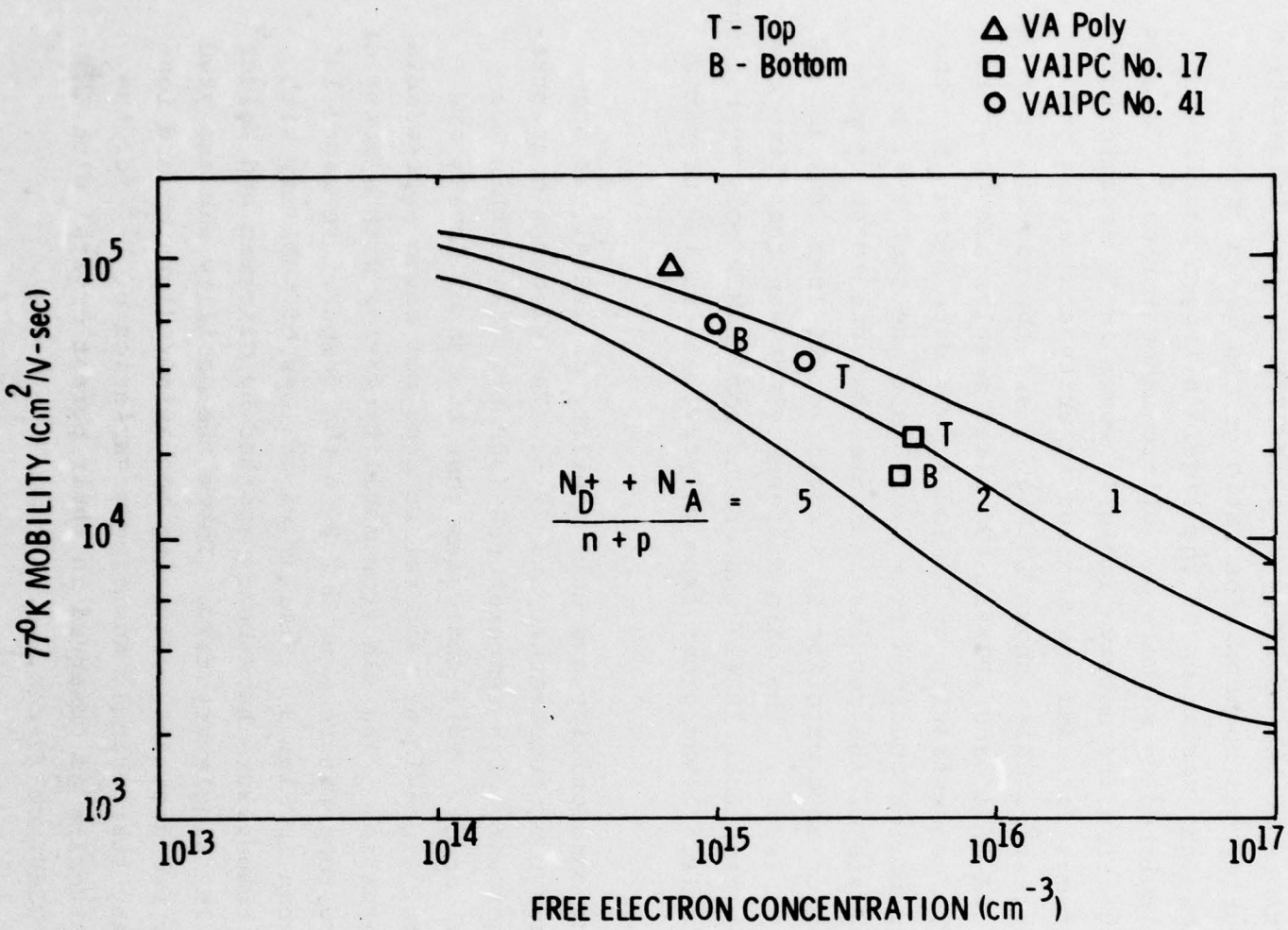

Fig. 8. Variation of LN mobility with free electron density showing a comparison of the experimental data points for different bulk grown n-type InP single crystals with theoretical predictions for three different $N_D^+ + N_A^-/n+p$ ratios (solid curves).

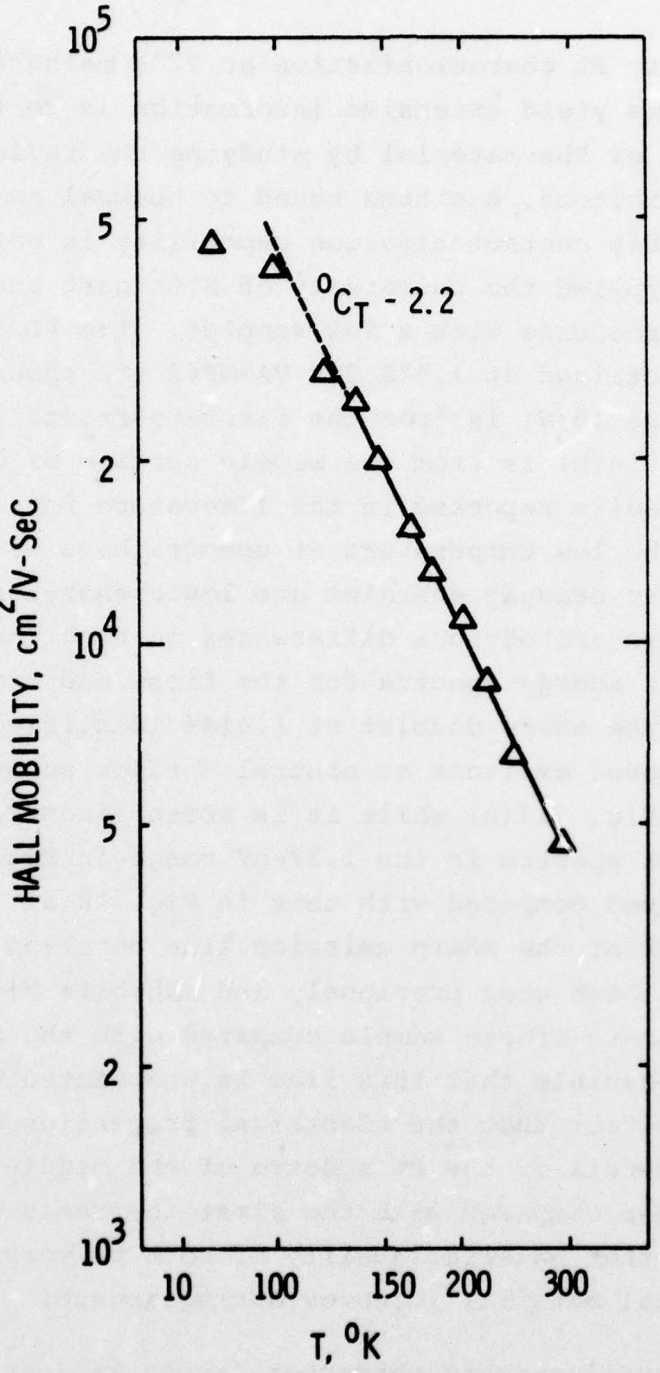

Fig. 9. Dark Hall mobility vs temperature for sample IPC#41.

In addition to PL characterization at 77°K measurements at lower temperatures yield extensive information as to the purity and stress state of the material by studying the radiative transitions of free excitons, excitons bound to neutral acceptors and donors. Since this characterization capability is not available at Varian, we supplied the University of Stuttgart and Wright-Patterson Air Force Base with a few samples. The PL results from Stuttgart obtained at 1.8°K for VA-GF#2 are shown in Fig. 10(a)-(b). Figure 10(a) is from the first-to-freeze sample of GF#2, while Fig. 10(b) is from the middle section of GF#2. Much like the results reported in the literature for InP epitaxial layers, the low temperature PL spectra have well-defined structures at near bandgap energies and lower energies centered at 1.38 eV. There are obvious differences in both the near-bandgap and lower energy spectra for the first and middle sections of GF#2. The sharp doublet at 1.4144 identified as recombination of bound excitons at neutral shallow acceptors is clearly seen in Fig. 10(b) while it is absent from Fig. 10(a). Similarly, the PL spectra in the 1.37-eV range in Fig. 10(b) are better resolved compared with that in Fig. 10(a). The only exception is that of the sharp emission line centered at 1.3605 eV which has not been seen previously and exhibits higher intensity in the first-to-freeze sample compared with the middle sample. It is possible that this line is associated with Si impurities. The fact that the electrical properties and the resolution and detail of the PL spectra of the middle section of GF#2 are higher compared with the first-to-freeze section is strong evidence that material quality of both polycrystalline and single-crystal material improves during growth.

Routine crystallographic characterization was carried out by optical microscopy in determining the etch pit density and how it was affected by variables such as doping species and doping density. A dislocation density etch originally reported

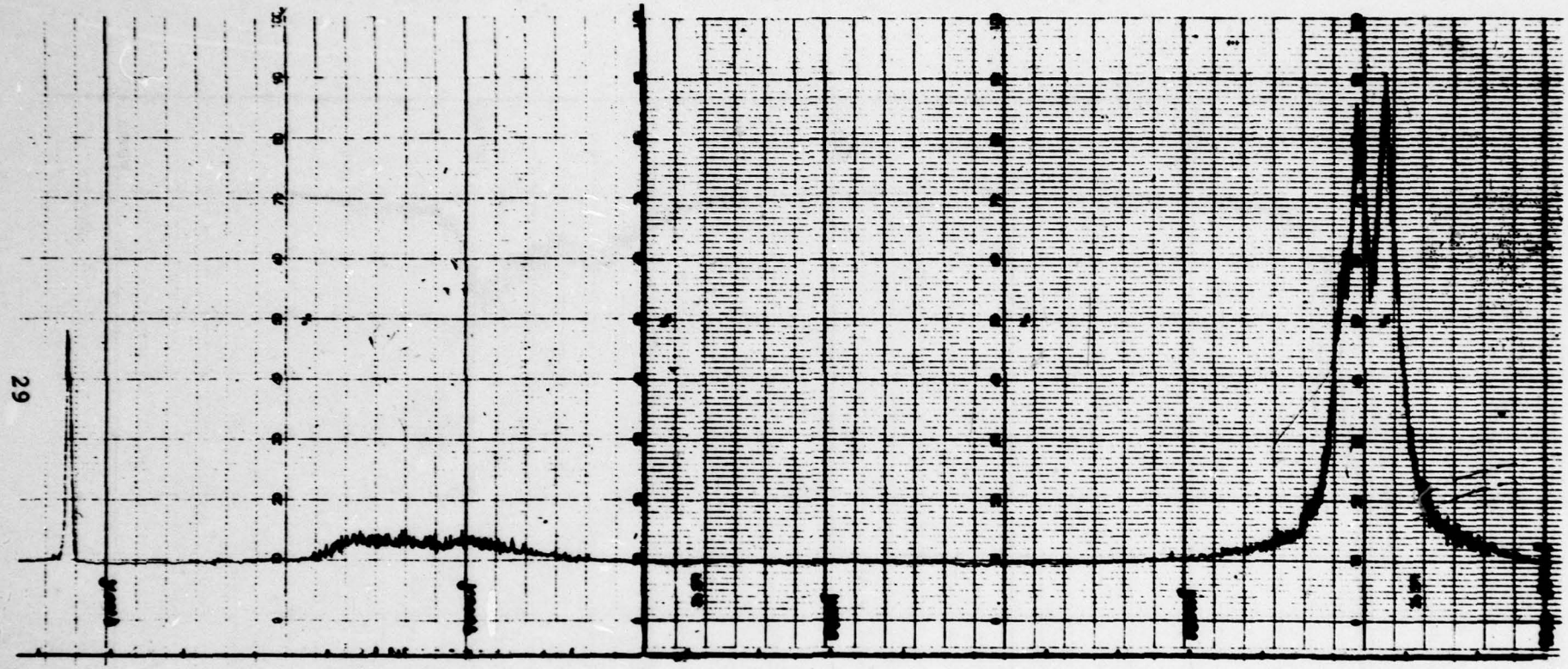

Fig. 10(a). Low temperature PL spectra of a "first-to-freeze" section of GF#2 polycrystalline solution-grown InP ingot.

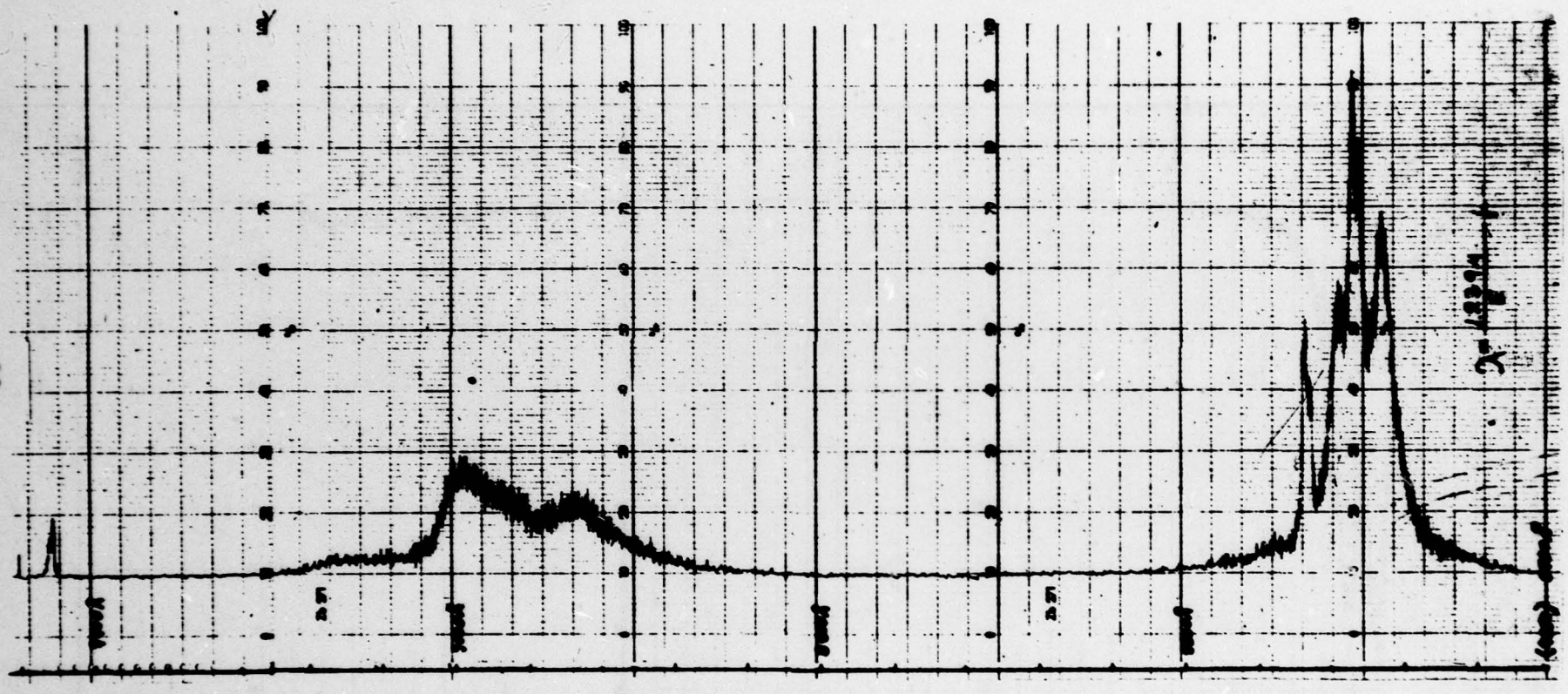

Fig. 10(b). Low temperature PL spectra of the middle section of GF#2 polycrystalline solution-grown InP ingot.

by Clark et al.[6] for (111)-oriented InP consisted of HCl, HNO_3, and Br. This etch produced well-developed pyramidal pits that were well correlated with dislocations as determined by x-ray topography. The reaction rate of this etch is extremely rapid and requires some experience in unambiguously determining dislocation densities. Figure 11(a) shows excellent delineation of dislocations in a low dislocation density substrate. For higher dislocation densities the etch pits normally coalesce, making accurate materials characterization difficult if not impossible. To overcome this limitation an etch that was used by Kuhn-Kuhnenfeld[7] (K-K) for GaAs and GaP and consisting of HF, H_2O_2, and H_2SO_4 was used with excellent results for InP. Figure 11(b) shows an InP wafer having moderate etch pit density. The wafer was originally etched in the Clark etch, showing the pit coalescence, and subsequently in the K-K etch pit. This picture shows the 1:1 correlation of the etches with respect to dislocation pit delineation, with the K-K etch being more selective in etching close to the vicinity of the dislocation. Using the K-K etch we expect to be able to determine the defect structure of the material in the vicinity of a precipitate. This can be seen in Fig. 11(c), where again the defect was delineated with the Clark and K-K etches. It is clear that the K-K etch shows a pile-up near a source of intense dislocations at a crystallographic defect, presumably a precipitate, while the Clark etch simply shows a multi-faceted etch pit.

Since it was reported by Seki et al.[8] that Zn doping in InP drastically reduces the growth in dislocation density, we initiated a series of experiments to investigate whether a similar effect is present with other dopants. Figure 12(a)-(d) is a series of low magnification photomicrographs of representative areas in wafers obtained from the top sections of InP crystals. In delineating the dislocations the wafers were initially polished with Br-methanol and subsequently etched in HF -H_2SO_4-H_2O_2

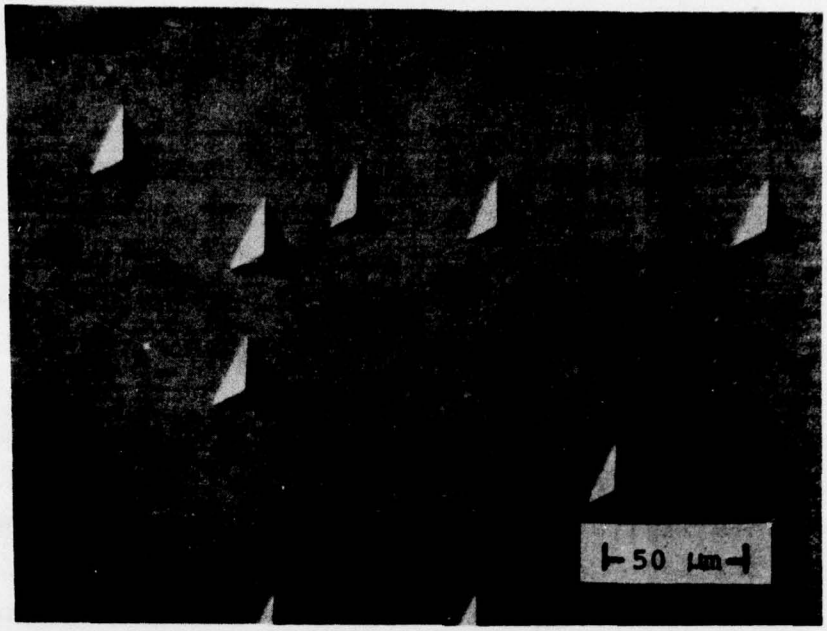

Fig. 11(b). Etch pit delineation of a low dislocation density InP wafer by HCl-HNO_3-Br etch.

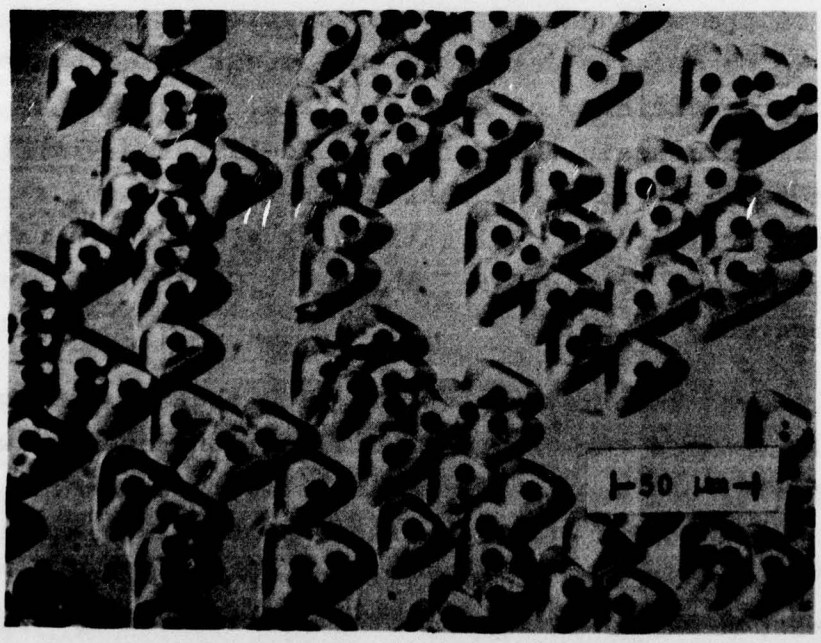

Fig. 11(a). Etch pit delineation of a moderate dislocation density InP wafer--large triangular pit obtained with HCl-HNO_3-Br etch, small dark pits obtained with H_2O_2-H_2SO_4-HF etch.

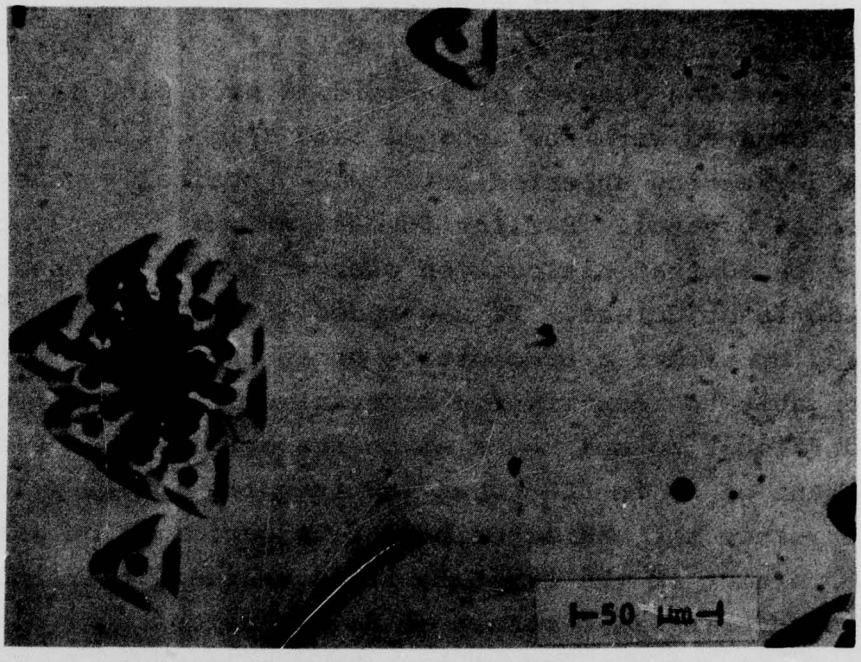

Fig. 11(c). Cluster of dislocations close to a precipitate or an inclusion--etched with both $HCl-HNO_3-Br$ and $H_2O_2-H_2SO_4-HF$ etches.

solutions. Figure 12(a) shows the dislocation density of crystal IPC#50 (undoped, n-type) having a background carrier concentration of 2×10^{15}/cc. The etch pits are well defined and have a density of $4 \times 10^{4}/cm^{2}$. For Sn-doped crystals of 2×10^{18}/cc carrier concentration the density of individual etch pits is drastically reduced compared with the undoped case (Fig. 12(b)); however, pronounced clustering appeared which was practically nonexistent in the undoped crystal. Earlier investigations by x-ray topography also indicated that dislocation clustering in Sn-doped InP was the predominant defect. It was speculated at the time that this is caused by either a precipitate or an inclusion. Since we have not been able to identify the material composition of the cluster, it is difficult to speculate as to its origin. The distribution coefficient of Sn in LEC-grown InP is quite low (2×10^{-3}). However, since the characterization is performed on wafers from the top portion of the crystal, it is unlikely that the dislocation clustering is a result of Sn inclusions. We plan to perform sputter Auger and microprobe measurements in order to identify the possible source of dislocation clustering in Sn-doped InP single crystals.

Figure 12(c) shows the dislocation density of a representative area of an Fe-doped wafer from the top portion of the crystal. Finally, a drastic demonstration of the effect of doping on the etch pit density in InP can be seen in Fig. 12(d) which shows an area containing only two etch pits. The dislocation density of this wafer is less than $100/cm^{2}$. This particular crystal is doped with Zn to a level of 2×10^{18}/cc. A model that has been proposed by Seki et al.[8] and appears to account for experimental observations is based on the single bond energies between impurity and host atoms. In the case of Zn, S, and Te in InP, the bonds between host atoms and donors (donor-substituted P atoms), and host atoms and acceptor (acceptor-substituted for In atoms) increase from 46.8 Kcal/mole for In-P to 94.2 Kcal/mole for Zn-P,

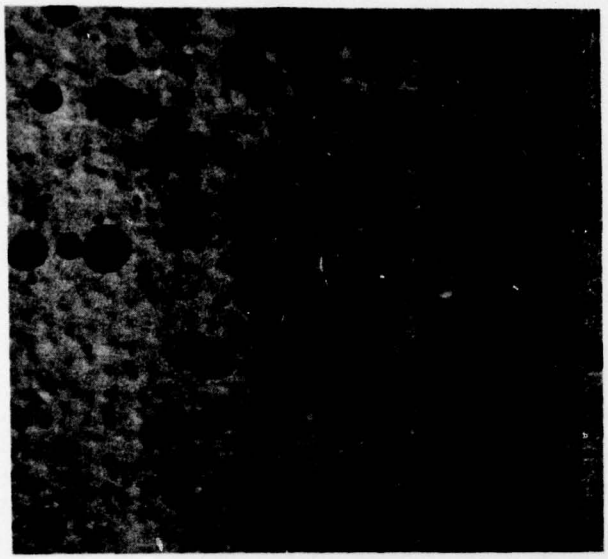

(a) Undoped (IPC#50).

(b) Tin-doped (IPC#51).

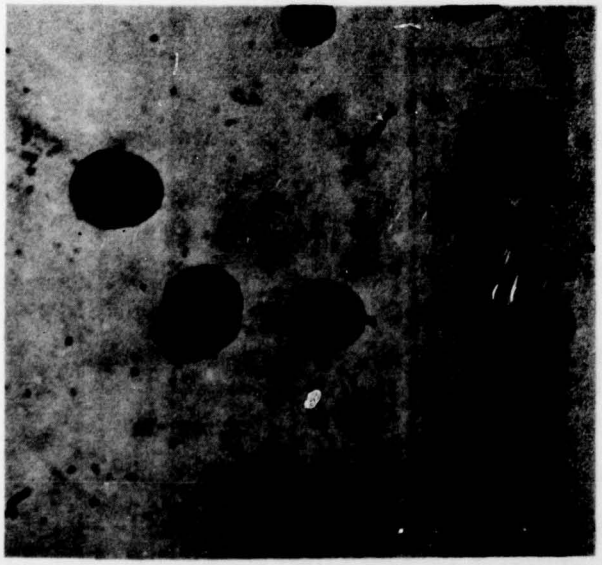

(c) Iron-doped (IPC#55).

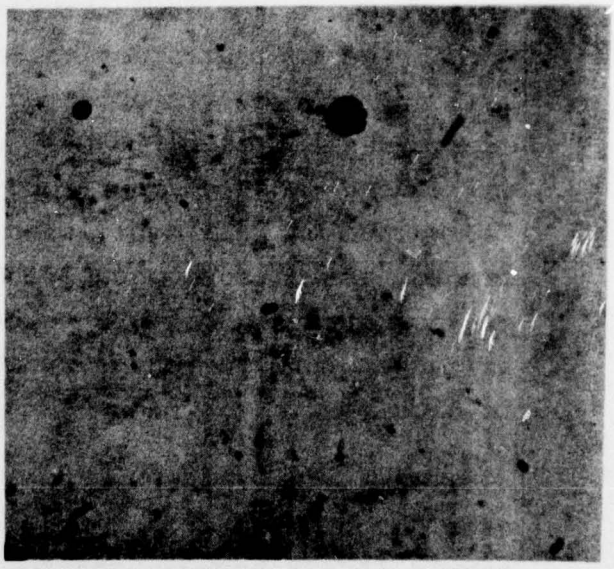

(d) Zinc-doped InP crystals (IPC#56).

Fig. 12. Low magnification (300x) photomicrographs of dislocation etch pits in representative areas of wafers.

68.7 Kcal/mole for In-S and 47.0 Kcal/mole for In-Te. This increase in single bond energy is thought to be responsible for the pinning of the dislocations that are normally generated at the periphery of the crystal, preventing them from propagating to the interior of the crystal.

The electrical properties of semi-insulating InP (Cr or Fe-doped) single crystals, grown by the LEC technique, have been reported by several investigators.[9-11] The thermal activation energies for Fe based on temperature-dependent resistivity measurements and for Cr based on temperature-dependent ohmic and space-charge-limited current were reported to be 0.66 eV and 0.54 eV below the conduction band respectively.

The dark conductivity and Hall effect for two Cr-doped InP crystals were measured between 320-200°K as shown in Fig. 13. For these samples an activation energy for electron density of 0.42 and 0.44 eV was obtained. For Fe-doped InP, an activation energy was estimated to be 0.62 eV below the conduction band, a value very close to that reported by Mizuno and Watanabe.[11] The dependence of Hall mobilities on temperature suggests that these samples are microscopically homogeneous (i.e. do not produce extra scattering centers to cause the decrease in Hall mobilities as temperature decreases, which is frequently observed phenomenon in high resistivity GaAs samples[12,13]).

Temperature-dependent Hall measurements confirm the presence of a donor level around 0.45 eV below the conduction band. In sample IPC#33 however the low temperature photoconductivity spectrum shown in Fig. 14 exhibits a long wavelength threshold level of 0.52 eV below the conduction band. This is presumably the same level reported by Pande et al.[10] and attributed to Cr. It seems that the resistivity properties of Cr and Fe-doped InP crystals are based on a four-impurity model: shallow donor and

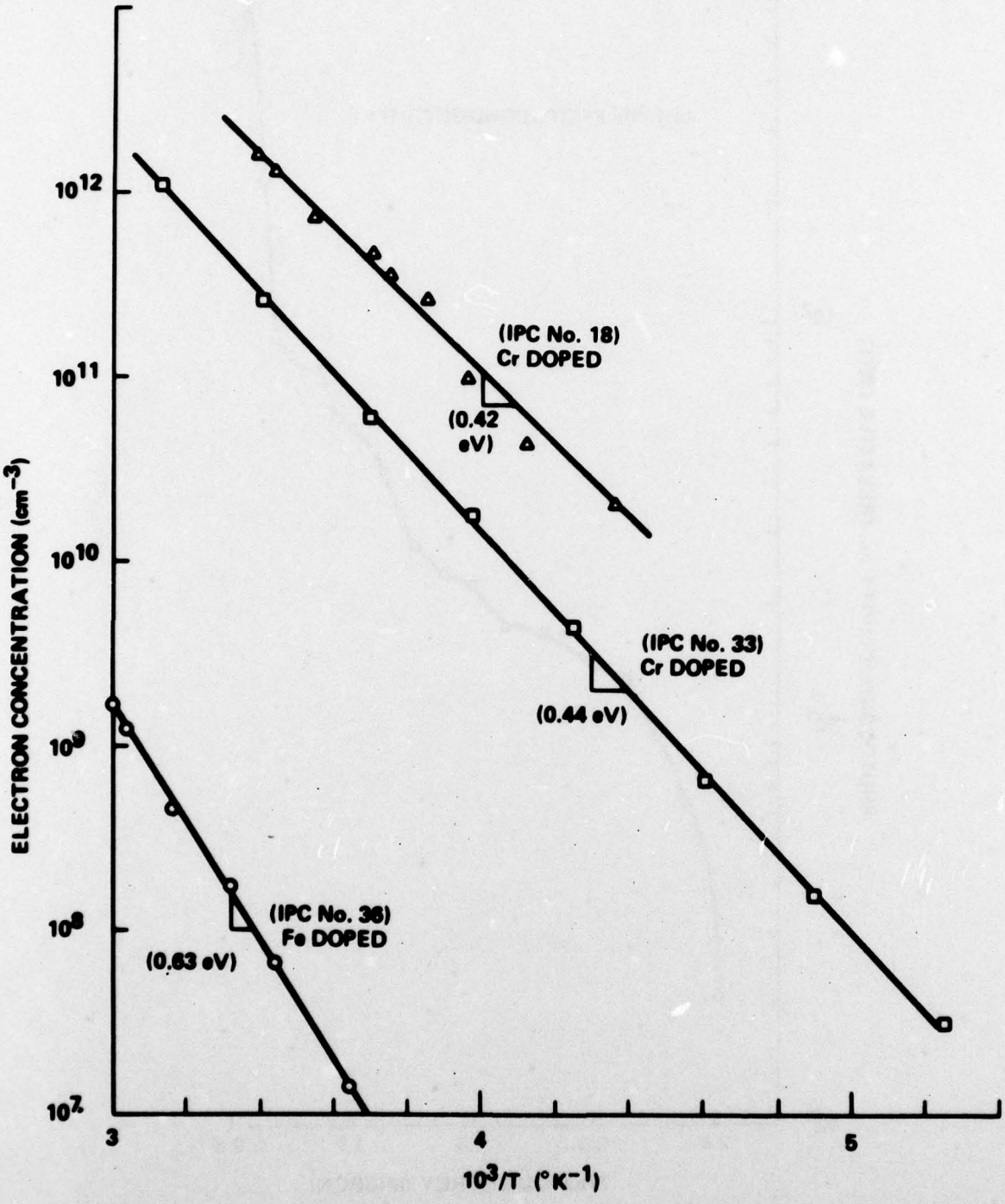

Fig. 13. Temperature dependence of n-type dark carrier density for one Fe-doped and two Cr-doped InP ingots.

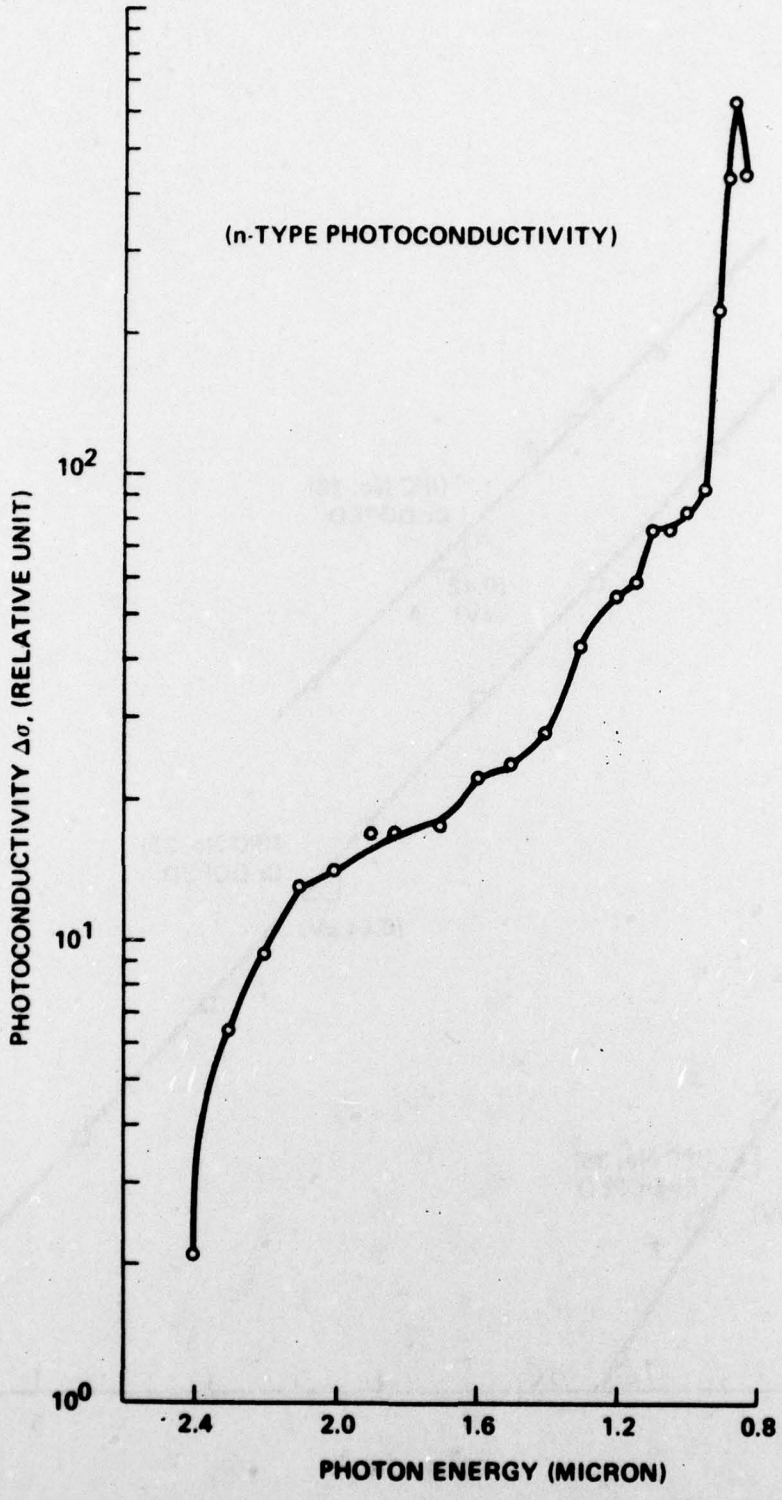

Fig. 14. Spectral response curve for the n-type photoconductivity on Cr-doped InP at 150°K.

acceptor and deep donor and acceptor. The shallow impurities are probably Si and Zn and deep impurities are O and Cr or Fe. An analysis based on the four-level model to explain the semi-insulating property of InP will be presented in the next report. A similar four-level model has been presented in the characterization of Cr-doped GaAs substrates by Zucca[14] and Lindquist.[15]

4. CONCLUSIONS AND RECOMMENDATIONS

The processes developed under this program for the growth of polycrystalline InP yield high purity material at a slow growth rate. Increase in the growth rate can be accomplished in the present system by increasing the In and P temperatures. This approach will be carefully tried so that the danger of explosions will be minimized. In addition, the effect of the higher reaction temperature on the electrical and photoluminescence properties of the crystals will be investigated.

For single-crystal growth the effect of doping on the defect density of the crystal could potentially become a powerful means to control the defect density. In particular, if isoelectronic impurities such as Ga and/or Al could be incorporated uniformly, low defect density InP crystals of any intentional doping level could become available. We plan to investigate the effect of isoelectronic impurities on the dislocation density during the next phase of the program.

5. REFERENCES

1. T. C. Harman, J. I. Genio, W. P. Allred, and H. L. Goering, J. Electrochem. Soc. 105, 731 (1958).

2. K. J. Bachmann and E. Buehler, J. Electron. Mater. 3, 279 (1974).

3. G. C. Baumann, K. W. Benz, and M. H. Pilkuhn, J. Electrochem. Soc. 123, 1232 (1976).

4. L. Eastman, private communication (1977).

5. M. Glickman and K. Weiser, J. Electrochem. Soc. 105, 728 (1958).

6. R. C. Clarke, D. S. Robertson, and A. W. Were, J. Mater. Sci. 8, 1349 (1973).

7. F. Kuhn-Kuhnenfeld in Proc. 1976 GaAs Conference (Inst. Phys. #33a, 1977), p. 158.

8. Y. Seki, J. Matsui, and H. Watanabe, J. Appl. Phys. 47, 3374 (1976).

9. J. B. Mullin, A. Royle, and B. W. Straughan in 1970 Symp. on GaAs (IPPS, London, 1971), p. 41.

10. K. P. Pande and G. G. Roberts, J. Phys. C: Solid State Phys. 9, 2899 (1976).

11. O. Mizuno and H. Watanabe, Electron. Lett. 11, 118 (1975).

12. A. L. Lin and R. H. Bube, J. Appl. Phys. 47, 1859 (1976).

13. A. L. Lin, E. Omelianovski, and R. H. Bube, J. Appl. Phys. 47, 1852 (1976).

14. R. Zucca, J. Appl. Phys. 48, 1987 (1977).

15. P. F. Lindquist, J. Appl. Phys. 48, 1262 (1977).

MISSION
of
Rome Air Development Center

RADC plans and conducts research, exploratory and advanced development programs in command, control, and communications (C^3) activities, and in the C^3 areas of information sciences and intelligence. The principal technical mission areas are communications, electromagnetic guidance and control, surveillance of ground and aerospace objects, intelligence data collection and handling, information system technology, ionospheric propagation, solid state sciences, microwave physics and electronic reliability, maintainability and compatibility.

Printed by
United States Air Force
Hanscom AFB, Mass. 01731